NUMERICAL STUDY OF INFLUENCE OF DEEP CORING PARAMETERS ON TEMPERATURE OF IN-SITU CORE

by

Hao WAN, Wu ZHAO, Xia HUA, Bo YU, Xin GUO, and Ling CHEN *

The School of Manufacturing Science and Engineering, Sichuan University, Chengdu, China

Original scientific paper
https://doi.org/10.2298/TSCI180813209W

The In-situ coring has a significant effect on the exploration of deep earth. However, in deep hard rock coring, the cutting heat in the process of coring generates high temperature and causes fidelity distortion of the in-situ core. Exploration of the mechanism of heat effect in the coring process is necessary to achieve the continuous control of temperature and obtain in-situ core. Due to the lack of systematic study on the surface and internal temperature rise of core samples during coring process, this paper uses the finite element simulation study the heat effect on the surface of the core under the influence of various cutting parameters. The numerical simulation results show that the surface of the core will not be burned under the cutting speed of 100 mm/s. At the condition of cutting speed 100 mm/s, feed rate 0.03 mm/r, thermal conductivity coefficient 1 W/m°C, the whole temperature rise will not exceed 1 °C. The interest results showed that cutting fluid has little effect on the temperature rise in the cutting process. If the requirement of core quality should avoid the pollution by drilling fluid, this study has supported the no drilling fluid for in-situ coring.

Key words: *deep, In-situ core, temperature, finite element simulation, cutting parameters*

Introduction

Many national long-term strategies of China and frontier sciences, such as underground space resources development, energy reserve, deep-earth mechanics, geophysics, microbiology and so on, were involved in the research of deep-earth resources [1, 2]. The deep mining environment, mechanical properties, and engineering responses of the rock mass were different from the shallow part [3, 4]. In order to retain the original characteristics of deep rock samples, the heat preservation requirement should be met in the mining of deep rock. At present, the soft rock in deep ocean with pressure coring was focused on in the core-taking technology of deep earth sampling [5]. However, in deep hard rock mining on land, the power consumption of core drilling was large, and most of the cutting work would be converted into cutting heat in the process of rock breaking [6, 7]. The heat generated was transferred into the core, which changed the physical properties and biological environment. Therefore, there was an urgent need to explore the mechanism of affecting temperature in coring process.

The factors affecting temperature rise and the ways to control temperature rise during drilling have been studied by a large number of scholars. In the process of cutting rock, an orthogonal experimental method to verify the blade temperature affected by parameters such

* Corresponding author, e-mail: chenlingscu@scu.edu.cn

as film heat dissipation coefficient, cutting speed and blade thickness was proposed in [8]. The heat transfer law of polycrystalline diamond compact (PDC) blade in rock cutting process and the heat distribution of the blade were analyzed in [9]. The temperature upon contact surface between a point-attack pick and the rock material by using a special thermocouple configuration was studied in [10]. The temperature of the cutter blade was focused more on in these studies, but the change of core temperature was paid less attention. The finite element simulation method to analyze the surface temperature of the core in cutting rock was presented in [11, 12], but there was lacked the research on the temperature change of the whole core. The heat transfer coefficient and the maximum temperature change of workpiece surface under the condition of approximate dry drilling was studied in [13], but whether this result was suitable for cutting rock must be further verification.

Heat transfer analysis of cutting process

Heat conduction is the main way of heat transfer in cutting process. It is assumed that the rock material is homogeneous and isotropic. Taking a circular section of a cylindrical core, the heat is transferred unidirectionally from a unit point on the circumference of the section the center of the circle. The 1-D heat conduction micro-volume element can be constructed.

In the process of cutting rock sample, elastic and plastic deformation of rock and friction with cutter will generate heat. The generated heat ΔQ in per unit time and area can be given [14]:

$$\Delta Q = \delta_c v_s \sin^2 \beta_0 + \sigma_n \mu v \cos \alpha_0 \tag{1}$$

Here, the part of the heat is transferred to the core, and the other conducts with the cutting fluid. Based on the Fourier heat transfer law and energy conservation law, a 1-D temperature field heat transfer control equation can be expressed [15]:

$$\frac{\partial}{\partial x}\left(\lambda_x \frac{\partial T_r}{\partial x}\right) + \Delta Q = \rho c \frac{\partial T_r}{\partial t} + \frac{\lambda P_s}{A_s}\left(T_r - T_l\right) \tag{2}$$

where the boundary condition is:

$$-\lambda_x \frac{\mathrm{d}T_r}{\mathrm{d}x} = \lambda\left(T_r - T_l\right) \tag{3}$$

Numerical model and simulation results

Geometric model

The cutting action of PDC blade on rock during drilling is simulated based on Deform 10.2 finite element software. The whole drilling process can be assumed to be a continuous and stable material deformation process. The deformation zone of drilling is concentrated on the contact part between cutting cutter tip and rock. In order to reduce the calculation and improve the authenticity of the results, the three blades cutting rock can be regarded as the single. The initial mesh number of workpiece is 12000, the ratio of maximum mesh size to minimum mesh size is 6:1. The initial mesh number of cutter is 10000, and the ratio of maximum mesh size to minimum mesh size is 4:1.

Material

Rock deforms elastically and plastically under high stress, and rock workpiece is set as elastic-plastic. Cutting tool is set as rigid body to reduce calculation. Taking sandstone as an example, the physical characteristics of rock and PDC cutter head are set as tab. 1.

Table 1. Physical properties of sandstone and PDC cutter

Material	Elasticity modulus [GPa]	Density [kgm^{-3}]	Thermal conductivity [Wm^{-1}°C^{-1}]	Heat capacity [JKg^{-1}°C^{-1}]	Poisson ratio
Sandstone	40	2650	3.5	800	0.25
Cutter	890	3510	543	790	0.07

The Johnson-Cook material model is used for cutting simulation. The Johnson-Cook model [16]:

$$Y = \left[A + B\varepsilon_0^n\right]\left[1 + C\ln\varepsilon^*\right]\left[1 - \left(\frac{T - T_{\text{room}}}{T_{\text{melt}} - T_{\text{room}}}\right)^m\right] \tag{4}$$

The values of the relevant parameters are shown in tab. 2.

Table 2. Values of Johnson-Cook material model parameters for rock

A	B	C	n	m	T	T_{room}	T_{melt}
1200	891	0.02	0.2	0.64	20	100	1527

Friction model and boundary conditions

The contact and friction model of cutting is established by using modified Coulomb friction law. The friction stress in the bonding zone can be regarded as a constant, and the friction stress in the sliding zone decreases along the cutting edge. The friction stress model [17]:

$$\begin{cases} f_s = \tau_m, & \text{while } f_s \geq \tau_m, (\text{bonding zone}) \\ f_s = \mu\sigma_n, & \text{while } f_s < \tau_m, (\text{sliding zone}) \end{cases} \tag{5}$$

The initial temperature of environment is set to 100 °C after calculating the gradient of ground temperature in 2000 m underground. In-situ formation water is used as drilling fluid for cooling and its conductivity coefficient is used to express the cooling intensity. Other parameters such as the front/rear shear angles cannot be changed in application. Therefore, the three parameters, cutting speed, feed rate and conductivity coefficient, are selected as simulation variables for orthogonal experiments.

Simulation results analysis

The simulation results show the temperature distribution in the cutting process, as shown in fig. 1. The highest temperature is located at the boundary between the chip and core. The parameters and simulation results set by orthogonal experiment method are shown in tab. 3. The experimental indexes corresponding to each factor are drawn as shown in fig. 2.

Table 3. Parameters and simulated maximum temperature

Cutting speed [mm·s^{-1}]	Conductivity coefficient	Feed rate [mm/r]	Maximum temperature [°C]
50	1	0.01	106
100	2	0.02	116
150	0.02	0.03	135
50	0.02	0.03	112
100	2	0.01	110
150	1	0.02	134
50	0.02	0.02	110
100	1	0.03	120
150	2	0.01	122

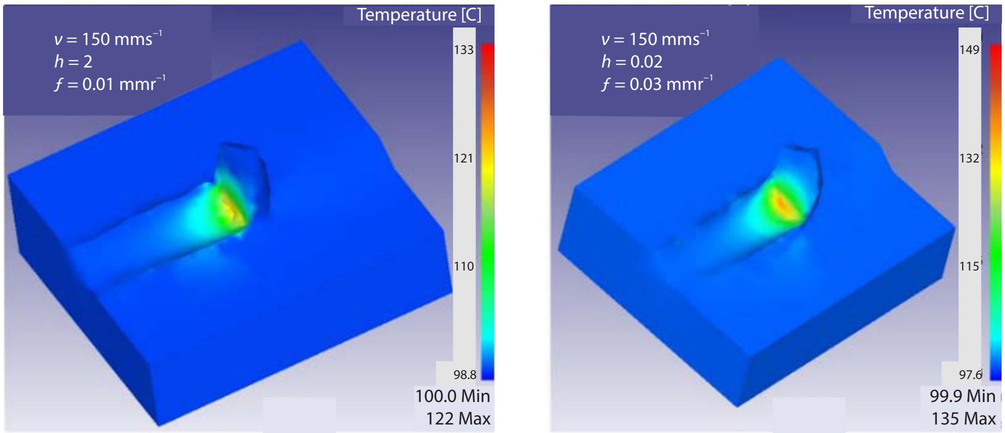

Figure 1. Temperature distribution under different parameter values

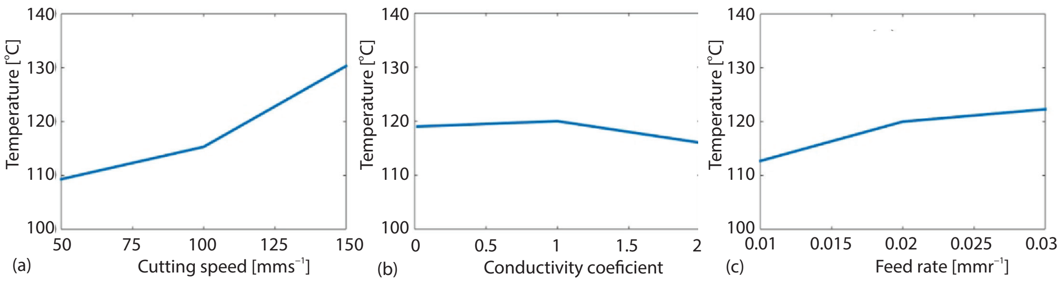

Figure 2. The relationships between cutting speed; (a) conductivity coefficient, (b) feed rate, and (c) the maximum temperature

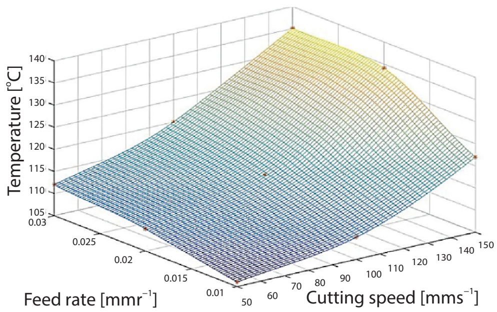

Figure 3. Comprehensive effect of cutting speed/feed on temperature

Comparing the range of the three factors, it can be concluded that the major factors affecting cutting temperature are cutting speed and feed rate compared with the conductivity coefficient. A fitted plane of the comprehensive effect of cutting speed and feed rate on temperature is shown in fig. 3. The slope of cutting speed direction is larger, so it has a greater influence on temperature than the feed rate. In practical engineering drilling, the feed rate is usually determined by the self-weight of the drilling rig and the resistance of the feed direction, and the adjustment ability is limited. So the cutting speed is the main adjustable factor.

Calculation of heat in cutting zone

Heat transfer analysis

The simulated temperature is the highest temperature of the core surface during drilling, which fails to reflect the change of the core internal and average temperature.

There are three deformation zones in cutting process. The heat in second deformation zone is mainly on the chips and cutting tools, which has little effect on the core and can be ignored. The heat transferred into the core comes from the first and third deformation zone, *i. e.* the shear and flank surface. The mechanical heat on the shear surface and the friction heat on the flank face can be written [14]:

$$L_a = \tau_s h_c h_w \sqrt{v_s^2 + \left(\frac{fv}{2\pi r}\right)^2} \sin\beta_0 \tag{6}$$

$$L_b = 0.5\tau_s h_w l_w \sqrt{v^2 + \left(\frac{fv}{2\pi r}\right)^2} \cos\alpha_0 \tag{7}$$

respectively.

The ratios of heat generated by shear face and flank face to the core can be given [17]:

$$R_1 = 1 - \frac{1}{1 + 1.33\sqrt{\dfrac{\lambda_r \varepsilon}{v h_c}}} \tag{8}$$

$$R_2 = \frac{\sqrt{\text{Pe}}(\tan\beta_0)^{0.1}}{\sqrt{\text{Pe}}(\tan\beta_0)^{0.1} + 0.24JK^{0.3}(\sin\alpha_0)^{0.1}} \tag{9}$$

respectively.

The heat transferred from the first zone and the third zone to the core are and, respectively. However, the heat transferred from the first shear zone to the core surface is cut into chips in a short time. Only a small part of the area near the cutter tip has a temperature effect on the final core. The heat in this small part can be expressed [17]:

$$Q_{ra} = \frac{L_a R_1}{h_c \csc\beta_0} = R_1 \tau_s h_w \sqrt{v_s^2 + \left(\frac{fv}{2\pi r}\right)^2} (\sin\beta_0)^2 \tag{10}$$

The total heat transferred into the core per unit time in the cutting process:

$$Q_r = R_1 \tau_s h_w \sqrt{v_s^2 + \left(\frac{fv}{2\pi r}\right)^2} \left(\sin\beta_0\right)^2 + 0.5R_2 \tau_s h_w l_w \sqrt{v^2 + \left(\frac{fv}{2\pi r}\right)^2} \cos\alpha_0 \tag{11}$$

The heat generated during the cutting process remains on the surface of the core. The heat will be transferred to the formation water and core center simultaneously, and the conduction ratio is determined by the thermal conductivity of both. The core heat allocated per unit volume is given:

$$Q = \frac{1}{\dfrac{v}{2\pi r}\pi r^2} \frac{Q_r \lambda_r}{\lambda_r + \lambda_w} \tag{12}$$

The relationship between overall temperature rise and cutting speed, feed rate and thermal conductivity coefficient is established:

$$\Delta T = \frac{Q}{c\rho} = F\left(v, \lambda, f\right) = \text{A}v^{1+\text{B}} \frac{1}{\text{C} + \lambda} \sqrt{1 + \frac{f^2}{\text{D}}} \tag{13}$$

where A, B, C, and D are constants, determined by the cutter parameters and material properties.

Calculations of temperature rise of rock sample

According to the cutting parameters in tab. 3, the shear stress obtained by simulation analysis at each level is shown in tab. 4. Combining shear stress with other parameters shown in tab. 5, the average temperature rise of the core after drilling and coring is obtained by calculation. Figure 4 shows the relationships between temperature rise and cutting speed in the case of abundant formation water cooling and a small amount of formation water approximating air cooling.

Table 4. Shear stress under cutting parameters in tab. 3

Number	1	2	3	4	5	6	7	8	9
τ_s [MPa]	1390	1550	1420	1440	1480	1420	1470	1410	1660

Table 5. Relevant parameters of core temperature rise formula

h_c	h_w	d	γ_0	α_0	l_w	c	r	φ	λ_r	λ_w	λ_a
2	28	6	0	9.37	1.242	800	25	0.57	2.864	1.6	0.023

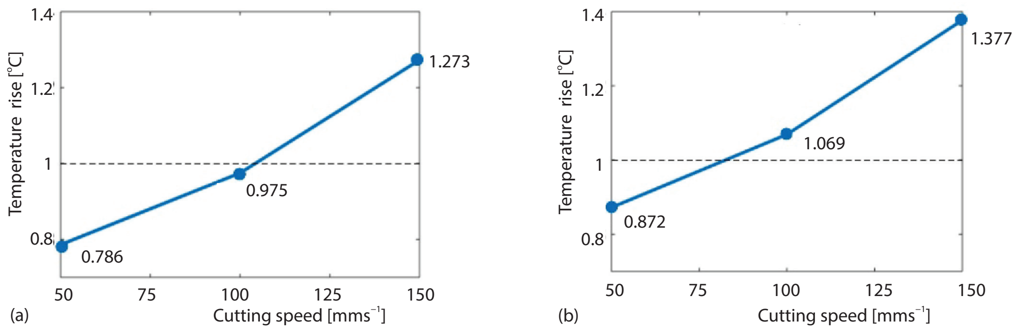

Figure 4. Relationships between temperature rise and cutting speed; (a) water cooling, (b) air cooling

Conclusion

In the present work, the influence of heat generation in coring on surface and temperature rise of cores were investigated. The numerical simulation results show that the cutting speed is the main factor affecting core temperature. Besides, how to improve the cutting efficiency under the minimum cutting speed and feed rate remain to be further studied.

Acknowledgment

This work was financially supported by the National Natural Science Foundation of China (Grant No. 51822403, 51674170), National Science Foundation for Young Scientist of China (Grant No. 51805340).

Nomenclature

A – initial yield stress, [Pa]
A_s – area of the section, [m^2]
B – hardening constant, [Pa]
C – strain rate constant, [–]
c – specific heat capacity, [Jkg^{-1} °C^{-1}]
d – blade thickness, [mm]
f – feed rate, [mm]
f_s – friction stress, [Pa]
h_c – cutting thickness, [mm]
h_w – cutting width, [mm]
J – correlation number, [–]
K – correlation number, [–]
l_w – contact length, [mm]
m – thermal softening exponent, [–]
n – hardening exponent, [–]
Pe – Peclet number, [–]
P_s – perimeter of the section, [m]
r – core radius, [mm]
T – reference temperature, [°C]
T_1 – ttemperature, [°C]

T_{melt} – melting temperature, [°C]
T_r – temperature of rock, [°C]
T_{room} – ambient temperature, [°C]
v – cutting speed, [mms^{-1}]
v_s – shear velocity, [mms^{-1}]
Y – effective yield stress, [Pa]

Greek symbols

α_0 – cutter back angle, [rad]
β_0 – shear angle, [rad]
γ_0 – cutter rake angle, [rad]
δ_c – shear strength, [Pa]
ε – relative slip coefficient, [–]
ε_0 – effective plastic strain, [–]
ε^* – normalized effective plastic strain rate, [–]
λ – thermal conductivity, [Wm^{-1}°C^{-1}]
λ_a – thermal conductivity of air, [Wm^{-1}°C^{-1}]
λ_r – thermal conductivity of rock, [Wm^{-1}°C^{-1}]
λ_w – thermal conductivity of water, [Wm^{-1}°C^{-1}]
λ_x – thermal conductivity along X, [Wm^{-1}°C^{-1}]
μ – friction coefficient, [–]
ρ – density, [kgm^{-3}]
σ_n – normal stress, [Pa]
τ_m – maximum shear stress, [Pa]
τ_s – shear stress, [Pa]
φ – friction angle, [rad]

References

[1] Pathegama, G. R., *et al.*, Opportunities and Challenges in Deep Mining: A Brief Review, *Engineering, 3* (2017), 4, pp. 250-261
[2] Liu, J., *et al.*, History, Advancements, and Perspective of Biological Research in Deep-Underground Laboratories: A Brief Review, *Environment International, 120* (2018), 1, pp. 207-214
[3] Klotz, A. R., The Gravity Tunnel in a Non-Uniform Earth. *American Journal of Physics, 83* (2015), 3, pp. 231-237
[4] Gao, M., *et al.*, Field Experiments on Fracture Evolution and Correlations between Connectivity and Abutment Pressure under Top Coal Caving Conditions, *International Journal of Rock Mechanics and Mining Science, 111* (2018), 2, pp. 84-93
[5] Magagnoli, M., A New Coring Method in Deep Water, *Marine Georesources and Geotechnology, 34* (2016), 4, pp. 496-503
[6] Wasantha, P. L. P., *et al.*, Do Joint Geometrical Properties Influence the Fracturing Behaviour of Jointed Rock an Investigation through Joint Orientation, *GeoMechanics and Geophysics for Geo-Energy and Geo-Resources, 1* (2015), 1-2, pp. 3-14
[7] Cui, J., *et al.*, Prediction of the Temperature of a Drill in Drilling Lunar Rock Simulant in a Vacuum, *Thermal Science, 21* (2017), 2, pp. 51-51
[8] Prakash, V., *et al.*, Temperature Distribution in Synthetic Diamond Cutters during Orthogonal Rock Cutting, *SPE Drilling Engineering, 4* (1989), 2, pp. 137-143
[9] Che, D., *et al.*, Analytical Modelling of Heat Transfer in Polycrystalline Diamond Compact Cutters in Rock Turning Processes, *Journal of Manufacturing Science and Engineering, 137* (2015), 3, 031005
[10] Shao, W., *et al.*, An Experimental Study of Temperature at the Tip of Point-Attack Pick during Rock Cutting Process, *International Journal of Rock Mechanics and Mining Sciences, 107* (2018), 3, pp. 39-47
[11] Rojek, J., Discrete Element Thermomechanical Modelling of Rock Cutting with Valuation of Tool Wear, *Computational Particle Mechanics, 1* (2014), 1, pp. 71-84
[12] Loui, J. P., Karanam, U. M. R., Heat Transfer Simulation in Drag-Pick Cutting of Rocks, *Tunnelling and Underground Space Technology Incorporating Trenchless Technology Research*, *20* (2005), 3, pp. 263-270
[13] Jiang, F., *et al.*, Estimation of Temperature-Dependent Heat Transfer Coefficients in Near-Dry Cutting, *International Journal of Advanced Manufacturing Technology*, *86* (2016), 5-8, pp. 1207-1218
[14] Shaw, M. C., *Metal Cutting Principles*, Clarendon Press, Oxford, UK, 1989
[15] Chen, W. C., *et al.*, Determination of Temperature Distributions on the Rake Face of Cutting Tools Using a Remote Method, *International Communications in Heat and Mass Transfer, 24* (1997), 2, pp. 161-170
[16] Johnson, G. R., Cook, W. H., Fracture Characteristics of Three Metals Subjected to Various Strains, Strain Rates, Temperatures and Pressures, *Engineering Fracture Mechanics, 26* (1985), 1, pp. 31-48
[17] Gui, W. Q., *High Speed Machining Technology* (in Chinese), National Defense Industry Press, Beijing, 2003

Paper submitted: August 13, 2018
Paper revised: November 11, 2018
Paper accepted: February 1, 2019

© 2019 Society of Thermal Engineers of Serbia
Published by the Vinča Institute of Nuclear Sciences, Belgrade, Serbia.
This is an open access article distributed under the CC BY-NC-ND 4.0 terms and conditions